

An RF Bunch Length Monitor for the SLC Final Focus*

F. Zimmermann, G. Yocky, D. Whittum, M. Seidel,
P. Raimondi, C.K. Ng, D. McCormick, K. Bane
Stanford Linear Accelerator Center
Stanford University, Stanford, CA 94309, USA

In preparation for the 1997 SLC run, a novel RF bunch-length monitor has been installed in the SLC South Final Focus. The monitor consists of a ceramic gap in the beam pipe, a 160-ft long X-band waveguide (WR90), and a set of dividers, tapers and microwave detectors. Electromagnetic fields radiated through the ceramic gap excite modes in the nearby open-ended X-band waveguide, which transmits the beam-induced signal to a radiation-free shack outside of the beamline vault. There, a combination of power dividers, tapers, waveguides, and crystal detectors is used to measure the signal power in 4 separate frequency channels between 7 and 110 GHz. For typical rms bunch lengths of 0.5–2 mm in the SLC, the bunch frequency spectrum can extend up to 100 GHz. In this paper, we present the overall monitor layout, describe MAFIA calculations of the signal coupled into the waveguide based on a detailed model of the complex beam-pipe geometry, estimate the final power level at the RF conversion points, and report the measured transmission properties of the installed waveguide system.

*Presented at the 1997 Particle Accelerator Conference (PAC97),
Vancouver, B.C., Canada, May 12–16, 1997*

*Work supported by the U.S. Department of Energy contract DE-AC03-76SF00515.

AN RF BUNCH-LENGTH MONITOR FOR THE SLC FINAL FOCUS*

F. Zimmermann, G. Yocky, D. Whittum, M. Seidel, P. Raimondi, C.K. Ng, D. McCormick, K. Bane
Stanford Linear Accelerator Center, Stanford University, CA 94309, USA

Abstract

In preparation for the 1997 SLC run, a novel RF bunch-length monitor has been installed in the SLC South Final Focus. The monitor consists of a ceramic gap in the beam pipe, a 160-ft long X-band waveguide (WR90), and a set of dividers, tapers and microwave detectors. Electromagnetic fields radiated through the ceramic gap excite modes in the nearby open-ended X-band waveguide, which transmits the beam-induced signal to a radiation-free shack outside of the beamline vault. There, a combination of power dividers, tapers, waveguides, and crystal detectors is used to measure the signal power in 4 separate frequency channels between 7 and 110 GHz. For typical rms bunch lengths of 0.5–2 mm in the SLC, the bunch frequency spectrum can extend up to 100 GHz. In this paper, we present the overall monitor layout, describe MAFIA calculations of the signal coupled into the waveguide based on a detailed model of the complex beam-pipe geometry, estimate the final power level at the RF conversion points, and report the measured transmission properties of the installed waveguide system.

1 INTRODUCTION

During the 1996/97 downtime of the Stanford Linear Collider (SLC), a novel RF bunch length monitor was installed in the South Final Focus, about 45 m away from the interaction point (IP). The monitor can detect the longitudinal distribution of both electron and positron bunches, which pass this point with a time separation of roughly 300 ns. It will permit control of the bunch length at the IP, which, due to bunch compression in the 1.2-km long collider arcs, can be very different from the bunch length that is measured in the SLAC linac, and may have a significant impact on the luminosity.

Previous attempts to commission a bunch-length monitor based on an RF cavity [1] at the same location failed, presumably because the crystal rectifiers used for converting the RF signal could not withstand the high radiation and electromagnetic noise level in the final-focus tunnel.

The suspected noise problem is overcome, if the RF signal conversion is performed outside of the beamline vault. For this purpose, we recently installed a 160-ft long section of WR90 (brass) waveguide, extending from the South final-focus tunnel through a 60-ft deep penetration to the Compton-laser shack South of the collider hall. As illustrated in Fig. 1, using waveguide filters and couplers, the RF signal is split into 4 different channels, which span the 4 frequency ranges 8–11.6 GHz, 11.6–19 GHz, 19–110 GHz

and 59–110 GHz. The RF power in each channel is measured with crystal rectifiers connected to gated ADCs, and the 8 signals so obtained (4 each for both the electron and the positron beam) are continually read out by the SLC control system. Figure 2 shows a photograph of the signal-processing unit being assembled.

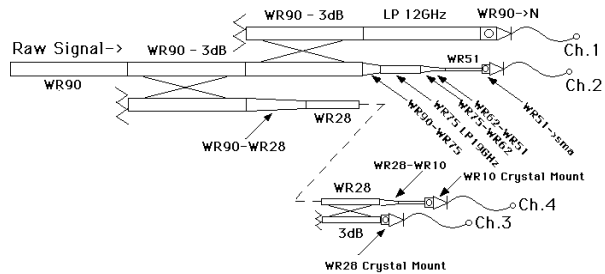


Figure 1: Schematic of RF signal processing.

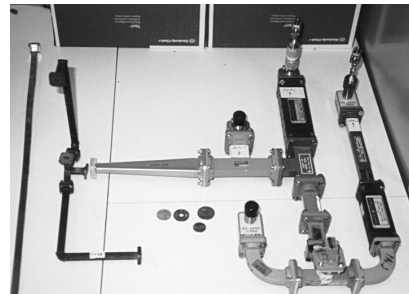


Figure 2: Assembly of signal-processing unit.

The signal detected in the different channels allows us to distinguish favorable and unfavorable bunch distributions at the interaction point. Beam-beam simulations with the code Guinea-Pig [2] were performed for different longitudinal distributions, as expected for small changes in the bunch-compressor (behind the damping rings) and linac set-ups [3]. Other beam parameters were assumed to be the same as in 1996. The simulations show that for bunches of rms length $\sigma_z \geq 1$ mm the luminosity is 30% higher than for 0.5 mm long bunches, due to the pinch effect (mutual focusing of the two beams during collision) [3]. The higher-frequency channels of our monitor are very sensitive to the bunch length: When the bunch length increases from 0.5 to 1 mm, the channel-4 signal is reduced by about 20 dB. For higher current and/or smaller horizontal IP spot size in 1997, the luminosity gain from bunch-length adjustment could approach 50–80%.

2 BEAM-WAVEGUIDE COUPLING

In the final-focus tunnel, the open-ended WR90 waveguide is pointed at a ceramic gap in the beam pipe; see photo-

* Work supported by the U.S. Department of Energy under contract DE-AC03-76SF00515.

graph in Fig. 3. This broadband pickup will be more versatile than a narrow-band cavity. Inner and outer radius of the ceramic are 1.5 cm and 1.9 cm, respectively. The total gap length is 4 cm, three quarters of which are occupied by a toroid. The waveguide is situated at the last free quarter of the gap and ends about 0.5 cm above the ceramic.

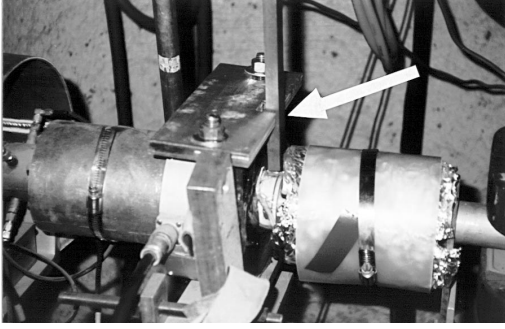


Figure 3: Waveguide pickup (arrow), toroid (left from waveguide), ceramic gap (below waveguide) and bellows (left and right), in the SLC South Final-Focus beam pipe.

The coupling of the radiated field into the waveguide was calculated for Gaussian bunches of different rms lengths, with the code MAFIA [4]. Figure 4 depicts the model of the beam-pipe geometry used in these calculations: The 0.5-cm wide gap between waveguide and ceramic is neglected, and the waveguide directly borders on the ceramic. The toroid is treated as a conducting boundary.

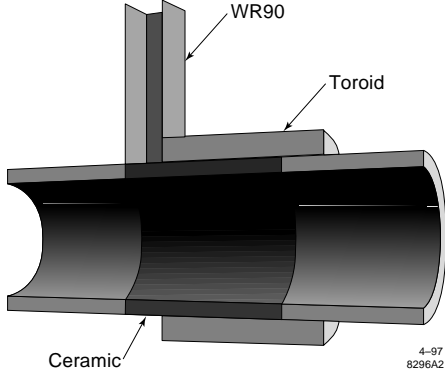


Figure 4: Model for the numerical calculation of beam-waveguide coupling using MAFIA [4].

The calculations show that the energy coupled into the TE_{10} mode is at least 2 times larger than that transmitted into the next important mode. Figure 5 illustrates the excitation of the TE_{10} mode by a 2-mm long Gaussian bunch as a function of frequency. Integration over time (or frequency) relates the signal a (or its Fourier transform \tilde{a}), that is computed by MAFIA, to the mode energy:

$$E_{TE_{10}} = \int |a(t)|^2 dt = \frac{1}{2\pi} \int |\tilde{a}(\omega)|^2 d\omega \quad (1)$$

Dividing the energy by the excitation time yields the RF power coupled into the TE_{10} mode. This is listed in the center column of Table 1.

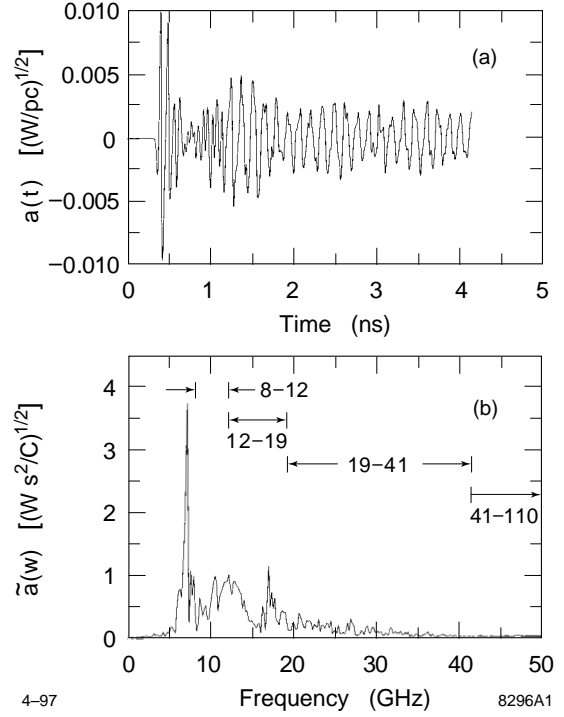


Figure 5: Signal $a(t)$ (in units of $W^{1/2}$) coupled into TE_{10} waveguide mode as a function of time, and its Fourier transform $\tilde{a}(\omega)$ (in units of $W^{1/2}s$) as a function of frequency, for a Gaussian bunch with 2 mm rms length.

3 WAVEGUIDE PROPERTIES

The interior broad dimension of the WR90 waveguide is $a = 2.286$ cm, which corresponds to a cutoff frequency $f_c = c/(2a) = 6.6$ GHz for the lowest (TE_{10}) mode. Using the skin depth $\delta_s \approx (2/(\omega\mu\sigma))^{1/2} \approx 4\mu/\sqrt{f(\text{GHz})}$, where σ denotes the conductivity and the numerical value applies to brass, the surface resistance is given by $R_s = 1/(\sigma\delta_s) \approx 15 \text{ m}\Omega \sqrt{f(\text{GHz})}$.

As the RF wave propagates through the waveguide, the power decreases exponentially from its initial value $P(0)$. After a distance s , the power in the TE_{10} mode is $P(s) = P(0) \exp(-2\alpha s)$, with an attenuation coefficient [5]

$$\alpha = \frac{R_s (2b\beta_c^2 + a\beta_0^2)}{Z_0 ab\beta_0\beta_z}, \quad (2)$$

where $Z_0 = 377 \Omega$, $b \approx a/2$ the small waveguide dimension, $\beta_c = \pi/a$, $\beta_0 = \omega/c$, and $\beta_z = (\beta_0^2 - \beta_c^2)^{1/2}$. Expressed in decibels the attenuation can also be written

$$A(s) [\text{dB}] = 8.686 \alpha s \quad (3)$$

At frequencies where the skin depth becomes comparable to the (unknown) surface roughness these formulae are no longer valid [5].

Figure 6 compares the measured attenuation of a signal reflected at the end of the 50-m long waveguide with the theoretical prediction of Eq. (3). At 10 GHz, the attenuation is about 7 dB for a wave propagating twice through the

entire waveguide, or about 0.2 dB per meter. This agrees well with the attenuation measured on a 12-ft long sample waveguide.

There are about 41 waveguide modes with a cutoff frequency below 50 GHz. The waveguide contains 11 H and E bends, at which part of the higher-frequency RF energy in the TE_{10} mode will be converted into other modes as the RF wave travels through the waveguide. In Fig. 6, the slight increase of the attenuation above 13 GHz may be due to excitation of the TE_{20} mode, whose cutoff frequency is 13.1 GHz.

Using the waveguide attenuation due to surface resistivity, given by Eqs. (2) and (3), assuming up to 10 dB additional attenuation due to conversion into other waveguide modes, and also including the two 3-dB couplers in the processing unit, we can roughly estimate the signal level at the crystal rectifiers, based on the power originally coupled into the TE_{10} mode. This estimate, shown in the right column of Table 1, is many 10's of dB above the noise.

Δf	init. power	est. signal
8–12 GHz	44 dBm	31 dBm
12 – 19 GHz	45 dBm	31 dBm
19 – 41 GHz	38 dBm	9 dBm
41 – 110 GHz	17 dBm	–22 dBm

Table 1: Power initially coupled into the TE_{10} waveguide mode and the estimated signal level, for a Gaussian bunch of rms length 2 mm and 4 different frequency ranges.

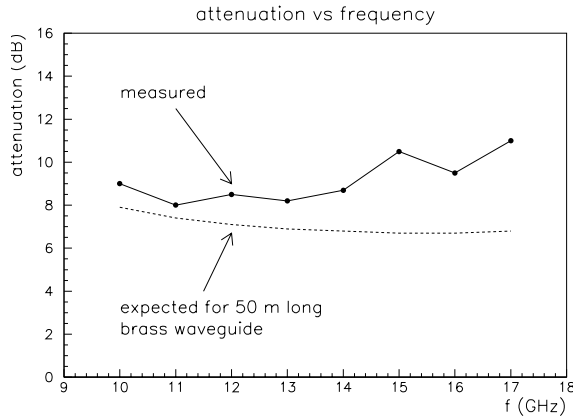


Figure 6: Measured attenuation of TE_{10} mode.

The group velocity in the waveguide is given by $v_g = c(1 - \beta_c^2/\beta_0^2)^{1/2}$ [5], and the propagation time over the distance $2L$ is simply $t_d = 2L/v_g$. Fig. 7 shows that, in the frequency range 7–12 GHz, the measured propagation times agree well with analytical expectation for a waveguide length L of about 50 m. For this measurement, the end of the WR90 waveguide was terminated with a reflecting plate.

The phase variation of the reflected RF wave as a function of frequency, $\Delta\phi(\omega)$, was measured with a mixer circuit combining the reflected and the drive signal. From

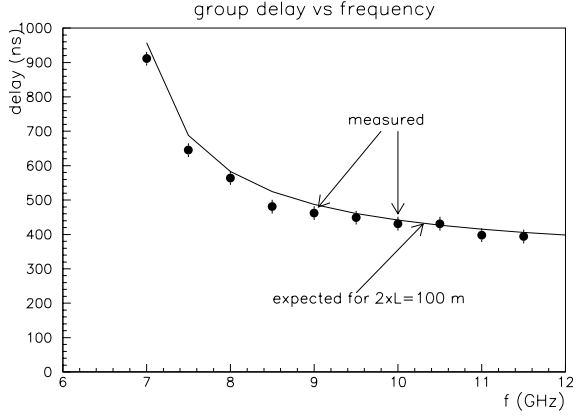


Figure 7: Measured and expected group delay for reflected TE_{10} mode in the ~ 130 -ft long WR90 waveguide, as a function of frequency.

this, and using the relation $L \approx c^2\beta_a/\omega(\Delta\phi/\Delta\omega)$, the electrical length of the waveguide was determined as $L \approx 49.24 \pm 0.03$ m, where the systematic error is probably much larger than the quoted statistical one.

Assuming power-detecting diodes, the crystal detectors mounted at the end of the waveguide measure the square of the electric field, and hence, their output voltage will be proportional to $V_{cr} \propto \sum_{k,l} E_k E_l^* e^{i(\phi_k - \phi_l)}$ where the sum is over all the modes above cutoff. If the length of the waveguide changes, e.g., due to temperature variation, the relative phase of two modes changes as well (in case of a temperature change ΔT , the phase of the i th mode changes by $\Delta\phi_i/\Delta T \approx (\beta_{ci}^2/\beta_{zi}^2 + 1)\beta_{zi}L\alpha \geq 0.2 \text{ K}^{-1}$ where $\alpha \approx 2 \times 10^{-5} \text{ K}^{-1}$ is the thermal expansion coefficient of brass, β_{ci} the cutoff frequency, and β_{zi} the propagation constant of the i th mode) and, as a consequence, so does the output signal. Since there are many modes, and since we average over wide frequency ranges, the sensitivity to length variation should be greatly reduced. More importantly, diurnal variations do not bar short scans of signal vs. compressor voltage or linac phasing, nor do they impede the continual comparison of electron and positron bunch lengths.

Acknowledgements

We thank M. Ross, M. Breidenbach and N. Phinney for support, A. Menegat, S. Tantawi and S. Hanna for helpful advice, and M. Woods for sharing the laser shack with us.

4 REFERENCES

- [1] E. Babenko et al., PAC93, Washington, p. 2423 (1993).
- [2] D. Schulte, private communication (1997).
- [3] K.L.F. Bane, P. Chen and F. Zimmermann, these proceedings (1997).
- [4] MAFIA RELEASE 3, DESY M-90-05K (1990).
- [5] R.E. Collin, Foundations for Microwave Engineering, McGraw-Hill, Singapore (1966).